INTERFACING A FLYWHEEL-BASED ENERGY STORAGE SYSTEM TO THE POWER UTILITY GRID THROUGH A SWITCHED RELUCTANCE MOTOR/GENERATOR

J. L. da Silva Neto[1], L. G. B. Rolim[2], G. G. Sotelo[3]
[1,2]DEE, UFRJ, Cidade Universitária, Rio de Janeiro, Brazil, e-mail : [1]luizneto@dee.ufrj.br, [2]rolim@dee.ufrj.br
[3] COPPE., UFRJ, Cidade Universitária, Rio de Janeiro, Brazil, e-mail: [3] sotelo@coe.ufrj.br

Abstract – **This paper presents a flywheel energy storage system, which uses a switched reluctance motor/generator, for custom power equipments. Two major potential applications are under consideration for further development: the compensation of voltage sags and a short-term uninterruptible power supply, to provide ride-through capability to critical loads under momentary fault or peak power conditions. The implementation of the control system was simulated with a commercial program.**

KEYWORDS

Energy storage system; power circuit control; SRM drive; energy quality.

I. INTRODUCTION

The current energy scenario in Brazil is calling for a global effort towards a more efficient use of electrical energy, as well as for a global improvement in the quality of its delivery. However, as budgets are limited, an acceptable alternative is the offering of different levels of supply quality, according to the concept of Custom Power, proposed by Hingorani in [1]. For the practical implementation of this concept, several types of equipment can be used, as described in [2]. Some of these equipments may employ some sort of energy storage device such as batteries or flywheels [3].

The above reasons have motivated the launch of a joint project between the Federal University of Rio de Janeiro (UFRJ) and a local energy distribution company, conceming the development of a flywheel-based energy storage device for custom power equipments. Two major potential applications are under consideration for further development: the compensation of voltage sags and a short-term uninterruptible power supply, to provide ride-through capability to critical loads under momentary fault or peak power conditions. With a flywheel system, energy can be drawn from the grid in a smooth way during periods of light system loading, imposing a minimum energy demand while the flywheel is accelerated. The energy can then be re-injected back into the network during peak load time periods, reducing the power delivered by the grid.

One significant aspect of the energy storage device is concerned to the electromechanical energy conversion between the flywheel and the electrical system to which it is connected. In this regard, it can be very advantageous if one and the same electrical machine is used not only to accelerate the flywheel when it is absorbing energy from the grid, but also for returning energy to the grid when the flywheel should operate as a generator. In high-speed flywheel systems, the mechanical and magnetic stresses imposed to the driving electrical machine are very high. For these reasons, the switched reluctance machine (SRM) can be pointed out as a good potential candidate for the intended application. There are several references in the literature [5-7] describing the application of SRMs as a reversible starter/generators for direct coupling to the shaft of aircraft engines. The main requirements for this kind of application are: *i)* Operation at very wide speed ranges from zero up to several ten thousand rpm; *ii)* Fault tolerance, in order to achieve a high reliability. Both requirements can be fulfilled by the SRM. Application of SRM in another kind of flywheel system has also been reported elsewhere [14].

The aim of this paper is to present the conception, mathematical modeling and simulation results of the control strategy to be applied to the power interface circuits for a SRM-based flywheel energy storage system.

II. SWITCHED RELUCTANCE MACHINE

The operation of a switched reluctance machine (SRM) is based on the principle of minimal reluctance. When the coil of some phase is excited, forces are developed over the magnetic circuit that tend to bring it to the position where the reluctance reaches a minimum, as seen from the energized coil. At this position coil inductance reaches a maximum. If this phase is switched off ant the next phase is switched on slightly before this position is reached, continuous movement of the rotor can be achieved. A six stator poles and four rotor poles (6/4 configuration) SRM have been used throughout this work.

The electromagnetic torque produced by one single coil is given by equation (1), where T_e is the torque, θ_r is the rotor angular position, λ is the total flux linked to the coil and i is the coil current.

$$T_e(\theta_r, i) = \frac{\partial}{\partial \theta_r} \int_0^i \lambda(\theta_r, i)\, di \qquad (1)$$

III. DYNAMIC MODEL OF THE SRM

Both relationships $T_e(\theta_r, i)$ and $\lambda(\theta_r, i)$ are strongly non-linear, a fact that makes it difficult to develop an analytical mathematical model for the SRM. Thus instead of trying to obtain such an analytical model, the methodology adopted in this work was to use tabulated data for $T_e(\theta_r, i)$ and $\lambda(\theta_r, i)$, which may have been obtained off-line by means of static measurements or FEM computations with the ANSYS [8] package, over a range of values wide enough to cover any situation that may occur within given simulation limits. The tabulated data is then used directly in the solution of the electrical and mechanical dynamic equations (1), (2) and (3). In equation (2), V is the coil terminal voltage, r_s is the coil resistance and i is the current flowing through the coil. In equation (3), J is the combined moment of inertia (SRM rotor plus flywheel), T_e is the electromagnetic torque and T_m is the opposing torque caused by mechanical losses.

$$V = r_s \times i + \frac{d(\quad_r, i)}{dt} \tag{2}$$

$$J \times \frac{d^2 \quad_r}{dt^2} = T_e \quad T_m \tag{3}$$

In order to carry out the simulations with PSCAD/EMTDC, the data tabulated in $\lambda(\theta_r, i)$ must be manipulated so a inverse relation $i(\theta_r, \lambda)$ could be produced. The phase inductance has to be modeled as current source controlled by the total flux linked to the coil and the rotor position, as shown in Fig. 1. The relationships $T_e(\theta_r, i)$ and $i(\theta_r, \lambda)$ are then integrated into standard 2-D lookup-table blocks, which use online linear interpolation to obtain intermediate values when needed. This model is very exact and can reproduce accurately the dynamics of the SRM when driven by a PWM power converter.

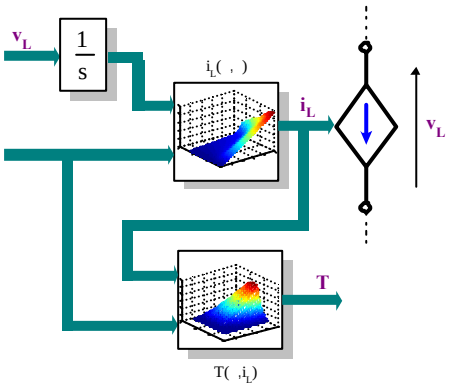

Fig. 1. The phase inductance of the SRM modeled in the PSCAD/EMTDC.

IV. FLYWHEEL ENERGY STORAGE SYSTEM

The main purpose of a flywheel device is to accumulate rotational kinetic energy, which can then be recovered to the electric system whenever is required. Many examples of flywheel-based energy storage systems are described in the literature, but they can be generally divided in two categories: low-speed, high inertia devices and high-speed, low inertia ones. In any case, in a time interval Δt the machine delivers (or absorbs) a quantity ΔEc of energy with an average power given by:

$$P = \frac{Ec}{t} = \frac{1}{2} J \frac{\left(\begin{smallmatrix} 2 & & 2 \\ 2 & & 1 \end{smallmatrix} \right)}{t} \tag{4}$$

V. APPLICATION IN A SHUNT COMPENSATOR

The use of an SRM flywheel with a shunt compensator is illustrated in Fig. 2, where the main system components can be identified, namely: bi-directional PWM power electronic circuits (the grid-side converter and the SRM driver); DC link; switched reluctance machine and flywheel. Depending on the voltage level at the grid side, a step-down transformer may be added between converter 1 and the system bus. As seen, the system operation is based on the injection of suitable currents. This topology can be employed in distribution systems to deal with loads that, for short periods of time, demand a considerable supplement of alternating real power ($\tilde{p}$) with frequency components less than the network fundamental, as: arc furnace; rolling mills; and during the acceleration of motors of great power.

A. Control strategy

The power electronics circuit consists of two converters. To drive the SR machine a half-bridge IGBT-based converter is used, allowing operation as motor or generator. The DC link is connected to the network by a bridge PWM converter, which is controlled according to Akagi's *pq* theory [13]. The objective of the control operation is to determine the direction of the power flow. This is achieved by regulating the DC link voltage. The flywheel shaft speed must be controlled according to the instantaneous active and reactive power demanded by the grid. In this work, the implementation of a two-stage control strategy for the flywheel shaft speed is proposed. Both stages are coupled through a common state variable: the voltage across the dc link capacitor. The main idea is to control the acceleration of the SRM in proportion to the mismatch between the dc link capacitor voltage and a given reference value, as depicted in the block diagram shown in Fig. 3. If no power flows between the flywheel and the grid, then the dc link capacitor voltage remains regulated at its nominal value. However, if active power is demanded by the grid, the command will act directly upon the network side converter, adjusting its current. Power flow control is performed through the direct-axis component of the converter output current at the grid side. The active power produced by this current is given by the internal product $v \cdot i + v \cdot i$ in the reference frame. It causes variation of the dc link capacitor voltage, which is compensated by the DC link voltage PI

regulator, which ultimately defines the operation of the machine as motor or generator. There is however another speed PI regulator (Fig. 4), with the main purpose of adding a small offset to grid converter average real power ($\bar{p}$), in order to bring the flywheel back to the rated maximum speed after any transients. Its output signal should be limited to values that do not cause excessive power consumption from the grid.

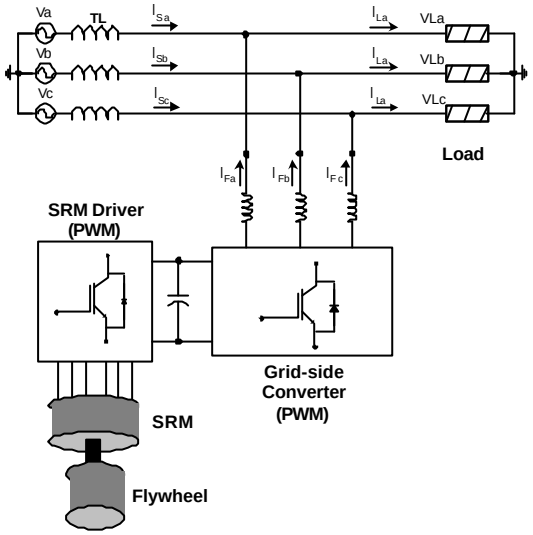

Fig. 2. Shunt compensator with an SRM flywheel.

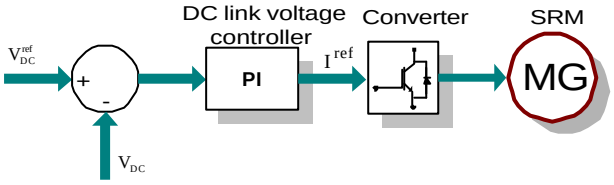

Fig. 3. DC link Voltage Control.

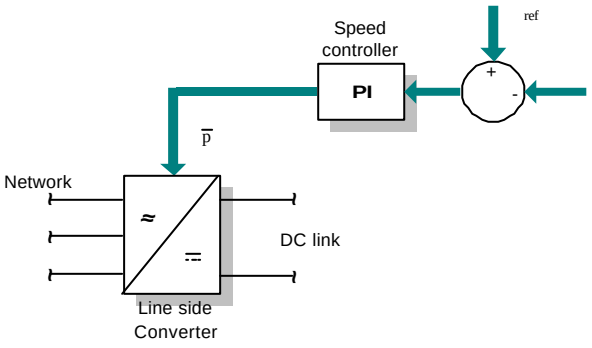

Fig. 4. Speed regulation.

B. The instantaneous power compensation algorithm

The compensation algorithm is based on Akagi's *pq* theory. The load voltages and currents are transformed into Clark components, and the instantaneous real power is calculated:

$$p_L = v_{La} i_{La} + v_{Lb} i_{Lb} \qquad (5)$$

By properly filtering, the part of the real power to be compensated ($\tilde{p}_L$) is extracted from the expression above. Then the currents to be synthesized are calculated as follows in coordinates:

$$\begin{matrix} i_F \\ i_F \end{matrix} = \frac{1}{v^2 + v^2} \begin{matrix} v & v \\ v & v \end{matrix} \begin{matrix} \tilde{p}_L + \bar{p} \\ 0 \end{matrix} \qquad (6)$$

C. Simulation Reults

The simulations presented in this paper have been carried out using the parameters of a low-power (1.5 kW), small-scale prototype machine, with a flywheel having an inertia of 0.065 kgm^2. A case of a 127V (L-N) network feeding a 4 kW load, have been studied. In t=0.25 s the load demands an extra 2 kW of real power with a duration of 200 ms (12 cycles). For this event the SRM operates delivering nominal power. In order to synthesize the shunt currents for the required torque, the DC voltage must be regulated in 400 V for a maximum rotor speed of 5000 rpm. Fig. 5 presents the load, shunt and source currents. The current on one phase of the SRM is shown in Fig. 6, while the total torque is presented in Fig. 7. It can be seen that the equipment operates as expected, injecting the correct currents (amplitude and phase) demanded by the increase in the load. This can be better observed in Fig. 8 where is shown: the power fractions delivered by the source and compensator; the total load power. Fig. 9 shows the DC link voltage regulated in 400 V with a transient variation of less than 1%. During the event simulated the grid-side converter drains energy from the DC link. The exact amount of energy drained is recovered with the regenerative breaking of the SRM, as seen in Fig. 10.

For a constant load, the power demanded from the generator is also constant. As the SRM decelerates, the electrical torque, and consequently its phase currents, must increase. However the current control is not affected, for the decreasing in speed enlarges the time interval in which each phase conducts, allowing the currents to reach their reference values. Fig. 11 presents a detailed view of the SRM phase and reference currents. It can be seen that for the simulated event conditions, that there are only two pulses for conducting phase.

Only the case of instantaneous real power compensation have been simulated. The shunt compensator, however, can also operate as a STATCOM or an active filter by introducing the desired power components to be compensated in the right side of the equation (6).

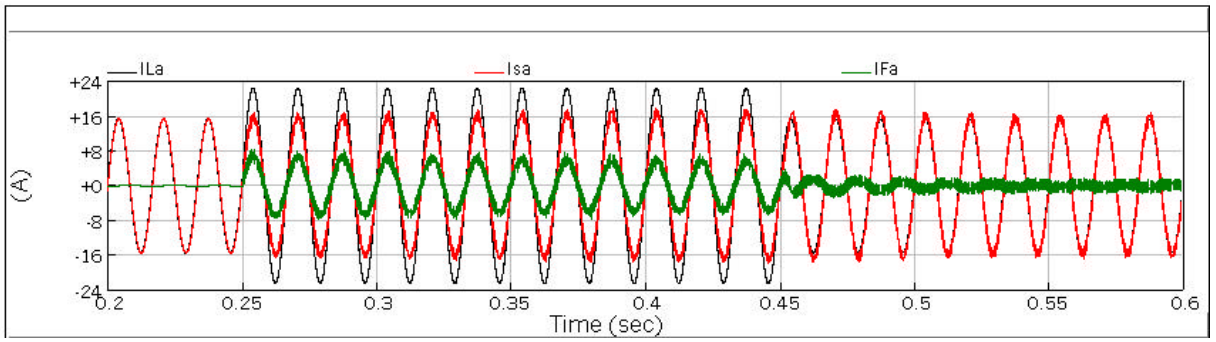

Fig. 5. Phase *a* currents: load (I_{La}); source (I_{sa}); shunt(I_{Fa}).

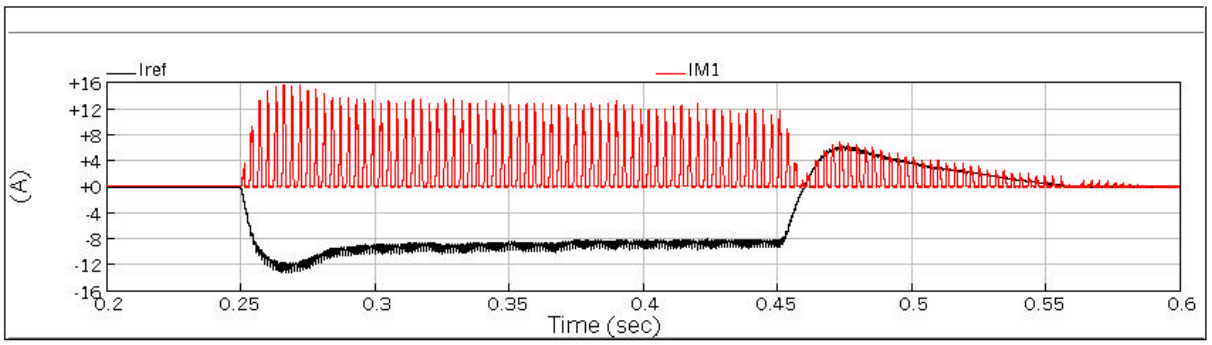

Fig. 6. Current in one phase of the SRM (I_{M1}) and its reference (I_{ref}).

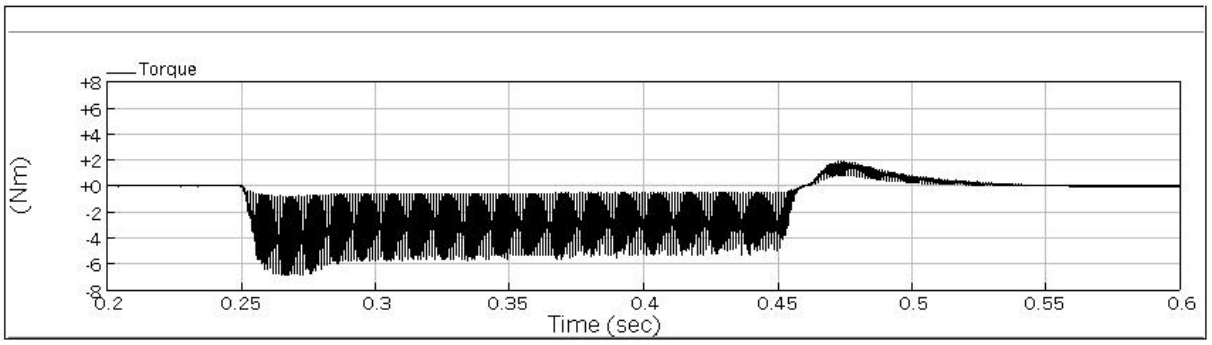

Fig. 7. Total SRM electrical Torque.

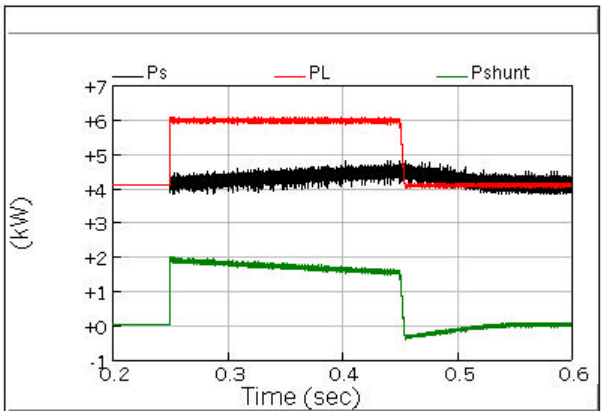

Fig. 8. The power fractions delivered by the source (P_s) and compensator (P_{shunt}); the total load power (P_L).

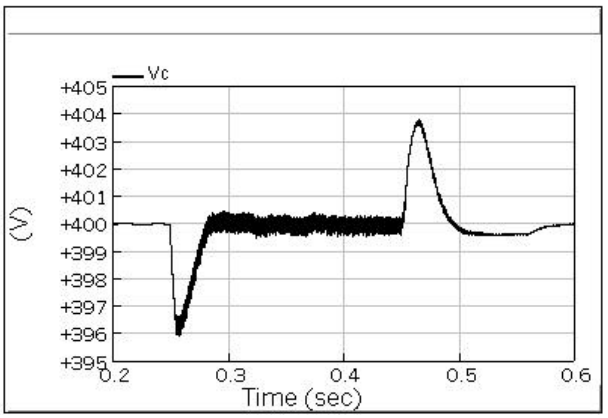

Fig. 9. The DC link voltage.

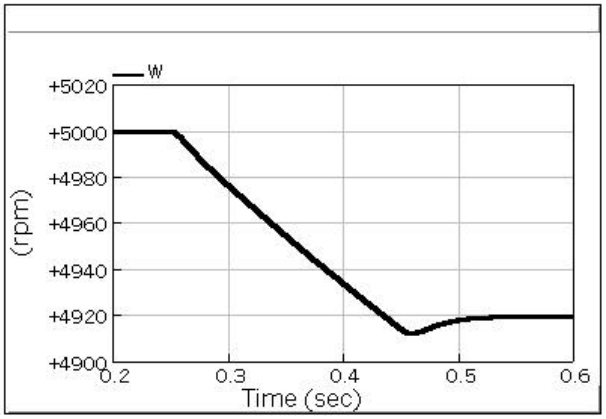

Fig. 10. The SRM speed.

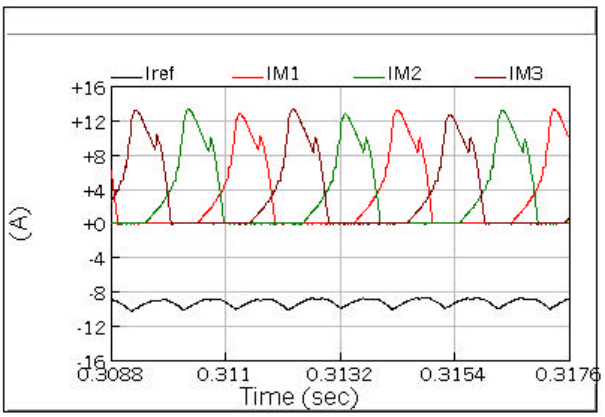

Fig. 11. Detailed view of the SRM phase and reference currents.

VI. APPLICATION IN A SERIES COMPENSATOR

A system with a DVR (Dynamic Voltage Restorer) [4] using the SRM flywheel is shown in Fig. 12. Its major objective is to deliver to a sensitive load, three-phase sinusoidal balanced and regulated voltages, even under voltage sags. The generated voltages are injected in the line through a series transformer. The control of the SRM drive is identical to the previous example.

Fig. 13 resumes the operations to control the grid-side converter in order to compensate voltage sags. A representative rms value of the load voltages is compared to a reference (1 pu) producing an error signal that is passed to a PI controller. The output of the PI is the modulation index (m_a) used in a Sine PWM control of the grid-side converter. In order to generate the references for the compensation voltages, unit-value rms voltages synchronized with the in-bus positive sequence voltages components are synthesized with the use of PLL algorithm.

A. Simulation Reults

At t = 0.3 s a three-phase fault during of 300 ms was applied at some point of the in-bu of the DVR, causing a voltage sag of 33%. Fig. 14 shows the voltages (phase A only) in the in-bus and out-bus of the DVR. On can observe that the equipment operates as expected keeping the load voltages regulated at their rated value. This fact is better seen in Fig. 15. Fig. 16 presents the regulated voltage on the DC link.

VII. CONCLUSIONS

Due to its elevated robustness and reliability, The SRM seems to be a good choice as a driving machine for flywheel energy storage devices. This work has presented the conception of an SRM flywheel system, considering both the mathematical modeling and control strategy. Two possible applications has been exemplified, where the use of such a kinetic energy storage system can contribute to the enhancement of power quality in electric energy systems. Magnetic losses can be reduced with an optimization of machine design and careful selection of core material. Windage and friction losses may be reduced using vacuum and a superconducting magnetic bearing [10][11][12].

VIII. REFERENCES

[1] N. G. Hingorani, “Introducing Custom Power”, IEEE Spectrum, pp. 41-48, June, 1995.

[2] R. Arnold, “Solutions to the Power Quality Problem”, IEE Power Engineering Journal, pp. 65-73, April 2001.

[3] G. Tanneau e D. Boudou, “Custom Power Interface”, Proceedings da CIRED2001, pp. 2.48, June 2001.

[4] Woodley, N. H., Sezi, T. (2001). New Design Dynamic Voltage Restorer (DVR™ MV) Systems, *IPEC’01 Conference,Singapore*, 17-19.

[5] C. A. Ferreira, S. R. Jones, W. S. Heglund and W. D. Jones, “Detailed Study of a 30-kW Switched Reluctance Starter/Generator for a Gas Turbine Engine Application”, IEEE Transactions on Industry Applications 31, 553-561 (1995).

[6] A. V. Radun, C. A. Ferreira and E. Richter, “Two-Channel Switched Reluctance Starter/Generator Results”, IEEE Transactions on Industry Applications 34, 1026-1034 (1998).

[7] M. E. Elbuluk, M. D. Kankam, “Potential Starter/Generator Technologies for Future Aerospace Application”, IEEE AES Systems Magazine, October 1996, pp. 17-24.

[8] Ansys Users Manual 2000.

[9] R. Hebner, J. Beno and A. Walls, “Flywheel Batteries Come Around Again”, IEEE Spectrum, pp. 46-51, April 2002.

[10] R. de Andrade Jr., A. Ripper, D. F. B. David and R. Nicolsky, “Stiffness and damping of an axial superconducting magnetic bearing”, *Physica C* **341-348**, 2607-2608 (2000).

[11] K. Atallah, Z.Q. Zhu and H.D. Howe, “The Prediction of Iron Losses in Brushless Permanent Magnet D.C. Motor, International Conference On Electrical Machines, Manchester. U.K., pp. 814-818, 1992.

[12] M.A. Mueller, S. Williamson, T.J. Flack, K. Atallah, B. Baholo, D. Howe and P. Mellor. “Calculation of Iron Losses from Time-stepped Finite-element models of Cage Induction Machines.”, 7th IEE Electrical Machines and Drives Conference, Durham, pp 77-81, 1995

[13] H. Akagi, Y. Kanazawa and A. Nabae, "Instantaneous Reactive Power Compensator Comprising Switching Devices Without Energy Storage Components," IEEE Transactions on Industry Applications, vol. IA-20, no. 3, 1984, pp. 625-630.

[14] I.J. Iglesias, L. Garcia-Tabares, A. Agudo, I. Cruz, L. Arribas, “Design and simulation of a stand-alone wind-diesel generator with a flywheel energy storage system to supply the required active and reactive power”, IEEE PESC 2000 Conference Proceedings, Volume: 3 , pp 1381–1386.

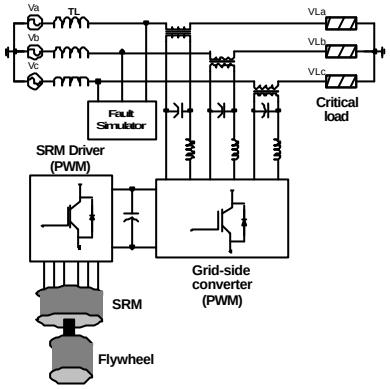

Fig. 12. DVR with Flywheel.

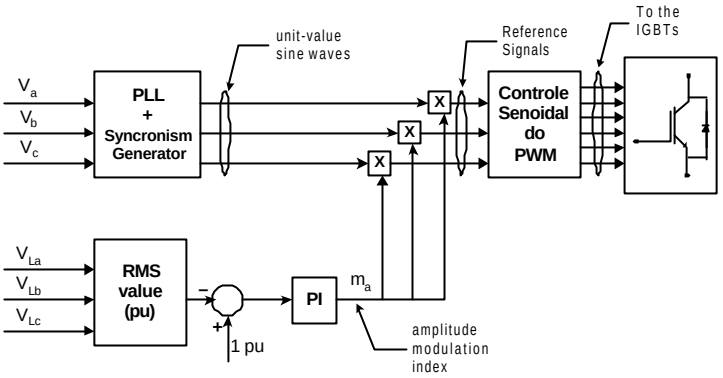

Fig. 13. Voltage sag compensation.

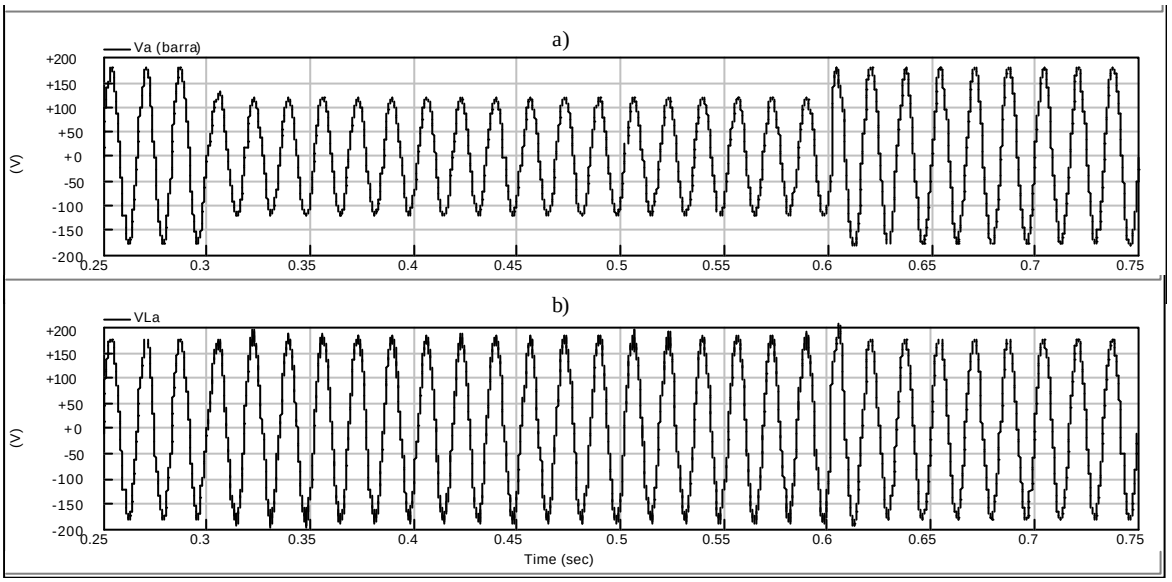

Fig. 14. Phase A voltages: a) at in-bus of the DVR; b) at the out-bus of the DVR (load voltages).

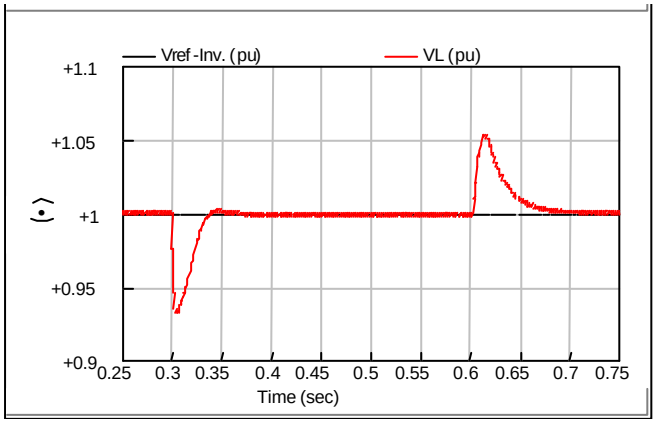

Fig. 15. RMS load voltage and its reference value.

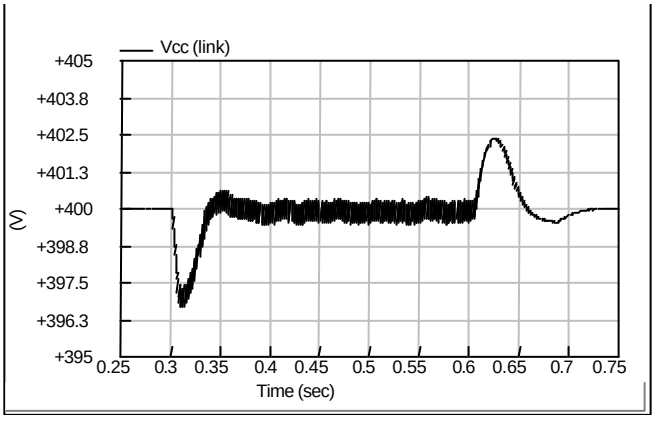

Fig. 16. DC link regulated voltage.